Two-step procedure to discriminate discordant from classical correlated or factorized states

Simone Cialdi [1,2], Andrea Smirne [3,4], Matteo G.A. Paris [1], Stefano Olivares [1], Bassano Vacchini [1,2]

[1] *Dipartimento di Fisica, Università degli Studi di Milano, Via Celoria 16, I-20133 Milan, Italy*
[2] *Istituto Nazionale di Fisica Nucleare, Sezione di Milano, Via Celoria 16, I-20133 Milan, Italy*
[3] *Department of Physics, University of Trieste, Strada Costiera 11, I-34151 Trieste, Italy*
[4] *Istituto Nazionale di Fisica Nucleare, Sezione di Trieste, Via Valerio 2, I-34127 Trieste, Italy*
(Dated: October 11, 2018)

We devise and experimentally realize a procedure capable to detect and distinguish quantum discord and classical correlations, as well the presence of factorized states in a joint system-environment setting. Our scheme builds on recent theoretical results showing how the distinguishability between two reduced states of a quantum system in a bipartite setting can convey important information about the correlations present in the bipartite state and the interaction between the subsystems. The two addressed subsystems are the polarization and spatial degrees of freedom of the signal beam generated by parametric downconversion, which are suitably prepared by the idler beam. Different global and local operations allow for the detection of different correlations by studying via state tomography the trace distance behavior between suitable polarization subsystem states.

The study of a bipartite system is an ever present theme which has led to important advancements in the understanding of quantum mechanics, especially when the two parties cannot be put on an equal footing. The prototypical situation is a measurement interaction, in which the interest is all on the side of the system, calling for tools and ideas allowing for an ever improving description of such interactions [1]. The theory of open quantum systems has provided a natural extension of these efforts, in which the quantum features of the measurement apparatus are put in major evidence [2], while correlations between system and environment have received important attention only more recently, thanks to the consolidation of quantum information theory [3]. The latest theoretical developments as well as the refinement in the experimental techniques has led to a change of paradigm in facing the system-environment (SE) dynamics. The possibility has been envisaged of actually exploiting the open quantum system, supposed to be liable to a relatively easy and accurate experimental observation, as a quantum probe of features of the environment, typically to be considered as a complex system. Properties of the environment which might be unveiled by an observation on the system up to now include the detection of quantum phase transitions [4], as well as the assessment of correlations within the state of the environment [5]. These advancements have been based on the study in time of the distinguishability of different initial system states [6], which has proven to be a fruitful strategy in order to exploit a quantum system as probe of features of a bipartite dynamics [7–13].

In this paper we improve this approach to devise a novel method for the determination of quantum correlations, which play a crucial role both in quantum information and in the development of quantum technologies. The approach is based on a two-step procedure, which relying on measurements on the system only allows to determine whether a given initial SE state actually contains quantum correlations, as quantified by quantum discord or, if this is not the case, decide whether it contains classical correlations or it is factorized. The relevance of this characterization lies in the fact that quantum discord has proven useful for different tasks in quantum information processing (see e.g. [14]). Our scheme goes beyond previous studies on the detection of initial correlations [7] and of quantum discord [10], takes as figure of merit for the distinguishability the trace distance among statistical operators [15] and is experimentally realized in an all-optical setup based on parametric downconversion (PDC) for the generation of correlations [16]. At variance with other approaches, relying on a measurement on multiple copies of the total system [17], we here only perform tomographic measurements on one of the subsystems.

Detection of correlations We start considering a SE state, which might contain correlations of some kind. For the experimental realization at hand we encode the system in the polarization degrees of freedom of one of the beams in the PDC (referred to as the signal). The environment corresponds to momentum (spatial) degrees of freedom of the signal, while the other beam (usually referred to as the idler) is exploited to prepare the initial state $\rho_{\mathrm{SE}}(0)$. In the first stage, the eigenstates of the reduced system state $\rho_{\mathrm{S}}(0) = \mathrm{Tr}_{\mathrm{E}}[\rho_{\mathrm{SE}}(0)]$ are obtained by performing state tomography. This allows us to define the two orthogonal projections on the system eigenstates, Π and $\mathbb{1} - \Pi$, and to introduce a dephasing operation Φ^d such that $\rho_{\mathrm{SE}}(0) \rightarrow \rho_{\mathrm{SE}}^d(0) \equiv \Phi^d[\rho_{\mathrm{SE}}(0)]$, where

$$\rho_{\mathrm{SE}}^d(0) = \Pi\rho_{\mathrm{SE}}(0)\Pi + (\mathbb{1} - \Pi)\rho_{\mathrm{SE}}(0)(\mathbb{1} - \Pi). \quad (1)$$

The dephased state has the same marginals of the initial one but, according to its expression, has zero quantum discord [18]. As suggested in [19], the difference between $\rho_{\mathrm{SE}}^d(0)$ and $\rho_{\mathrm{SE}}(0)$, as given by the trace distance, provides a quantifier of the quantum discord in the original state, namely:

$$T = \frac{1}{2}\|\rho_{\mathrm{SE}}^d(0) - \rho_{\mathrm{SE}}(0)\|_1 = \|\Pi\rho_{\mathrm{SE}}(0)\Pi - \frac{1}{2}\{\Pi, \rho_{\mathrm{SE}}(0)\}\|_1. \quad (2)$$

Now, one can prove the presence of non-classical correlations in $\rho_{\mathrm{SE}}(0)$ by just measuring the system. In fact, if quantum correlations are present the marginals of the system states after
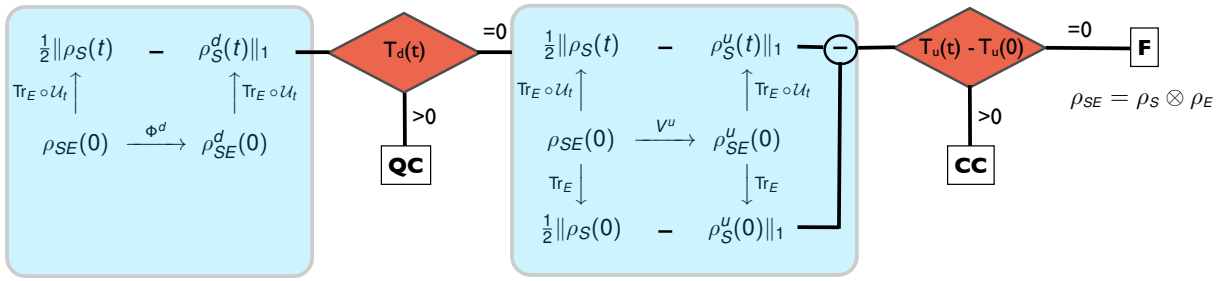
Figure 1. (Color online) Logical scheme of the cascading, two-step procedure exploited to discriminate among quantum correlated (QC), classically correlated (CC) or simply factorized (F) SE states. In the first stage (left box) a dephasing operation Φ^d which leaves invariant the marginals is applied, allowing to detect quantum correlations using as witness the trace distance $T_d(t)$ between the reduced states evolved from original and dephased state. If no quantum correlations are detected, the second stage (right box) is entered, in which the growth in time of the trace distance of initial states differing by a local unitary operation on the system V^u, i.e. $T_u(t) - T_u(0)$, allows to detect classical correlations or to conclude that the initial state is factorized. See the text for details.

a time evolution $\mathcal{U}_t$ will generally differ, even if coinciding at the initial time [10]. This implies that the quantity

$$T_d(t) = \frac{1}{2}\|\rho_S^d(t) - \rho_S(t)\|_1 = \left\|\mathrm{Tr}_E \circ \mathcal{U}_t[\rho_{SE}^d(0) - \rho_{SE}(0)]\right\|_1 \tag{3}$$

acts as a local witness of quantum discord in the initial state. This witness is probabilistic in nature, since not every time evolution is bound to reveal the existing quantum correlations. However, as argued in [11], the efficiency of the method is very high, and in the case considered a fixed time evolution allows for the detection of quantum discord in the whole range of states which can be prepared, apart from a set of measure zero. In the general case it has been shown that the average over the set of unitaries not only detects the quantum discord, but also allows to quantify it. This first stage of the detection scheme is described in the first section of the logical scheme in Fig. 1. If the witness provided by the expression Eq. (3) is positive, then the state $\rho_{SE}(0)$ does contain quantum correlations corresponding to non zero discord. On the other hand, if $T_d(t) = 0$, then the second stage of the cascading procedure is entered (second section in Fig. 1). At this level we have already checked the absence of quantum correlations, therefore we should perform a measurement involving only the system to check whether $\rho_{SE}(0)$ is a factorized state or contains classical correlations. Also in this case the presence of initial correlations can be unveiled by a growth of the trace distance between different initial states above the initial value as a consequence of the SE time evolution [7]: while the considered condition is in principle only sufficient, the considered time evolution allows to detect with unit efficiency the considered class of states. In order to generate another initial SE state without introducing correlations we perform a local unitary transformation denoted by V^u, which only affects the system degrees of freedom. Given the fact that the marginal states of the environment are left unchanged by V^u, the growth of the trace distance indeed witnesses the presence of initial correlations, rather than of different initial environmental states. We are then led to consider the behavior of the trace distance between the reduced system state ρ_S and its transformed counterpart ρ_S^u at the initial and at a later time. If the difference

$$T_u(t) - T_u(0) = \frac{1}{2}\|\rho_S^u(t) - \rho_S(t)\|_1 - \frac{1}{2}\|\rho_S^u(0) - \rho_S(0)\|_1 \tag{4}$$

which acts as correlation witness is greater than zero, then $\rho_{SE}(0)$ has classical correlations, otherwise the state is actually factorized, i.e. $\rho_{SE}(0) = \rho_S(0) \otimes \rho_E(0)$ (see Fig. 1).

Experimental realization In our experiment SE states with different correlations have been generated, and the two-step procedure described above for the discrimination of correlations has been tested, providing in particular an experimental verification of the scheme for the detection of quantum discord proposed in [10].

Our experimental apparatus, sketched in Fig. 2, is based on PDC generated by two 1 mm adjacent type-I Beta-Barium Borate (BBO) crystals, oriented with their optical axes aligned in perpendicular planes and pumped by a 10 mW, 405 nm
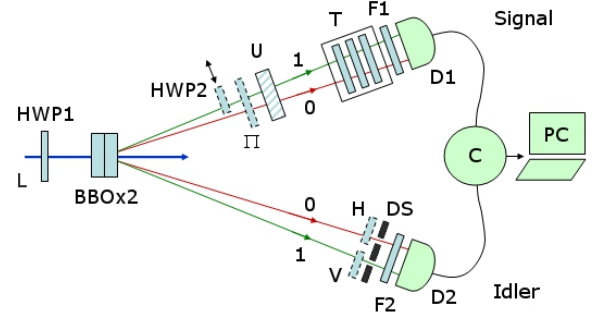

Figure 2. (Color online) Scheme of the apparatus. L is the pump laser, HWP1 and HWP2 are half-wave plates, BBOx2 two BBO crystals, Π a polarizer and U is the spatial light modulator. T is the tomographic scheme (a quarter-wave plate, a HWP and a polarizer), H and V denote two polarizers aligned along the horizontal and vertical axes, respectively, DS is the double slit, F1 a high pass filter (780 nm), F2 an interference filter (bandwidth of 10 nm and central wavelength of 810 nm); D1, D2 are detectors and C the coincidences counter. The components drawn with a dashed line have to be modified or moved according to the different stages of the procedure.

cw diode laser (Newport LQC405-40P). The two BBO crystals generate the signal and idler states with perpendicular polarization and the interference filter (F2) ensures a good spatial correlation between signal and idler [5, 20, 21]. We generate two channels 0 and 1 (corresponding to the momentum states $|0\rangle$ and $|1\rangle$, respectively) with a double slit (DS) positioned along the idler path. This scheme allows us to act on the idler beam to prepare the signal beam in the three cases of interest and to easily control and change the amplitude of the polarizations. The arrangement of the two BBO crystals produces a factorized state between polarization and momentum, namely $\rho_p \otimes \rho_m$. Both components are generally described by a mixture of the form [8] $\rho_k = P_k \rho_k^{\text{ent}} + (1 - P_k)\rho_k^{\text{mix}}$, where $k = p, m$, the statistical operator $\rho_k^{\text{ent}} = |\psi_k\rangle\langle\psi_k|$ denotes a pure entangled state and ρ_k^{mix} the corresponding mixed counterpart. The weight P_k is naturally interpreted as purity of the state, but does not play a role in the present treatment which studies the correlations between polarization and momentum. The states for polarization and momentum read $|\psi_p\rangle = \sqrt{\lambda}|HH\rangle + \sqrt{1-\lambda}|VV\rangle$ and $|\psi_m\rangle = \frac{1}{\sqrt{2}}(|00\rangle + |11\rangle)$ respectively, where H and V denote horizontal and vertical polarizations. The relative weight of the two polarization states parametrized by $0 \leq \lambda \leq 1$ can be adjusted at will by means of a half-wave plate (HWP) located in the path of the pump laser, while the balance in the momentum degrees of freedom is obtained by a careful alignment of the preparation apparatus and optimizing the phase-matching between the crystals. Controlled correlations between system (polarization) and environment (momentum) can be introduced inserting in the idler beam a horizontal and a vertical polarizer in the paths corresponding to the momenta denoted by 0 and 1 respectively. If no further operation is performed, the obtained state is of the form

$$\rho_{\text{SE}}^{\text{CC}} = \lambda|H\rangle\langle H| \otimes |0\rangle\langle 0| + (1 - \lambda)|V\rangle\langle V| \otimes |1\rangle\langle 1|, \quad (5)$$

which clearly exhibits only classical correlations, while states with non zero quantum discord are generated by inserting a half-wave plate (HPW2) in the momentum channel 1 of the signal beam, thus obtaining

$$\rho_{\text{SE}}^{\text{QC}} = \lambda|H\rangle\langle H| \otimes |0\rangle\langle 0| + (1 - \lambda)|\theta\rangle\langle\theta| \otimes |1\rangle\langle 1|, \quad (6)$$

where $|\theta\rangle = \cos(\theta)|H\rangle + \sin(\theta)|V\rangle$. In the left panel of Fig. 3 we plot the quantum discord in such a state as quantified by Eq. (2). The absence of polarizers in the idler path leads to take the trace over the idler degrees of freedom and therefore to the factorized state

$$\rho_{\text{SE}}^{\text{F}} = (\lambda|H\rangle\langle H| + (1-\lambda)|V\rangle\langle V|) \otimes \frac{1}{2}(|0\rangle\langle 0| + |1\rangle\langle 1|). \quad (7)$$

The eigenstates of the reduced system states, whose knowledge is necessary to determine the dephasing operation described in Eq. (1), that is the projections Π and $\mathbb{1} - \Pi$, are obtained through the full tomography (T) of the polarization states [22], as depicted in Fig. 2. The projections are implemented by means of polarizers according to the measured
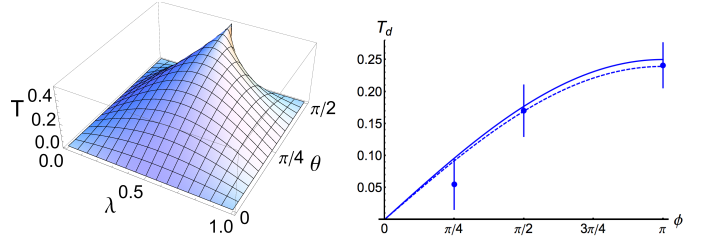

Figure 3. (Color online) (Left) The amount of quantum discord T defined in Eq. (2) for a state given in Eq. (6), as a function of λ and θ. (Right) Measured values of T_d for different values of the parameter ϕ, which describes the interaction between system and environment. The two points for $\phi = \pi/2$ and $\phi = \pi/4$ have been obtained for $\lambda = 0.5$, whereas for $\phi = \pi$ we have set $\lambda = 0.48$. The solid and dashed lines correspond to $\lambda = 0.5$ and $\lambda = 0.48$, respectively.

eigenstates. The interaction between system and environment is obtained by a spatial light modulator (U), which can insert a position and polarization sensitive phase in the signal. In particular we have realized an evolution corresponding to a phase-gate, acting on the momentum corresponding to channel 1 only by applying a phase to the polarization degrees of freedom according to the operator $\text{Diag}(e^{i\phi}, 1)$ in the $\{|H\rangle, |V\rangle\}$ basis. As shown in the right panel of Fig. 3, the optimal performance in the correlation detection is obtained for $\phi = \pi$, which has thus been taken as reference value. In the following, the time specification "0" will denote the state right after the preparation, while the time "t" will identify the state after the interaction. The unitary transformation V^u on the system degrees of freedom only, used to prepare the other reference state for the second stage of the two-step procedure of Fig. 1, is obtained by inserting a half-wave plate intercepting both momenta in the idler beam.

The experimental results are summarized in Fig. 4, that reports the data of the tomographic analysis. In the first row examples of the system-environment states corresponding to Eqs. (6), (5) and (7), respectively, are considered for specific values of λ and θ. From the tomographic data we retrieve the expression for the dephasing operation Φ^d to be implemented. In the second row the reduced system states after the time evolution corresponding to a phase gate are given, to be compared via trace distance with the reduced states plotted in the third row and obtained by applying Φ^d to the overall state before the evolution. The experimentally measured value of the trace distance growth corresponding to Eq. (3) is given in the fourth row. When this value is zero (within the experimental errors), thus pointing to the absence of quantum discord, a further analysis corresponding to the second stage of the scheme in Fig. 1 is performed. Therefore, we first apply a local unitary operation V^u to the system and then measure the quantity Eq. (4), whose positivity reveals the presence of correlations in the initial state, as detected by a growth of the distinguishability in time between different initial reduced system states. The experimental values for the quantity in Eq. (4) are given in the last row of Fig. 4, showing that indeed a factorized state
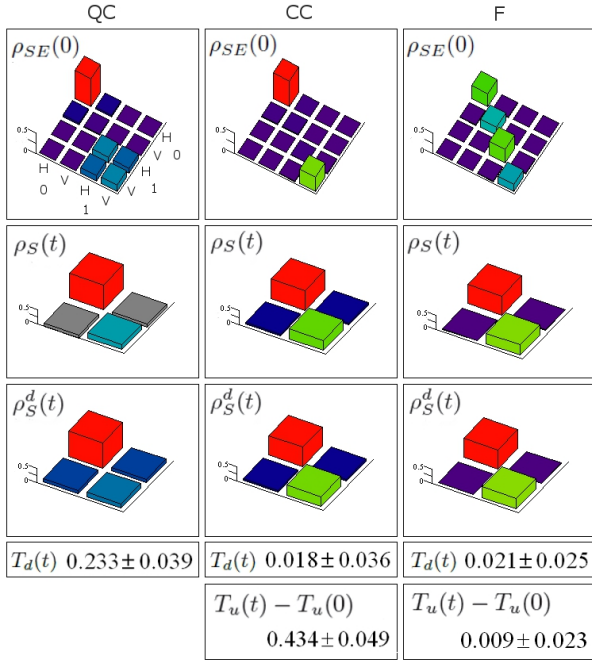
Figure 4. (Color online) Tomographic measurements of the states involved in the experiment. In the left column the case of a state of the form Eq. (6) with $\lambda = 0.7$ and $\theta = \pi/4$ has been considered. From top to bottom we have plotted the observed values for $\rho_{SE}(0)$, $\rho_S(t)$ and $\rho_S^d(t)$ respectively. In the central column we provide the corresponding measurements for the state Eq. (5) with $\lambda = 0.64$. The value $T_d(t)$ of the trace distance Eq. (3) is here compatible with zero according to the experimental error, testifying the absence of quantum discord, while the positivity of $T_u(t) - T_u(0)$ given by Eq. (4) shows the detection of classical correlations. In the right column the considered state corresponds to Eq. (7) with $\lambda = 0.65$, and the factorized structure of the state is unveiled by the value of $T_u(t) - T_u(0)$, which is zero within the experimental value. The time specification 0 and t denote the states right after the preparation and the interaction stages respectively.

can be detected within the experimental accuracy. In fact the indistinguishability of two statistical operators corresponding to zero trace distance can be consistently assessed within a tomographic approach since quantum tomography is a statistically reliable procedure, meaning that for any finite number of repeated preparations one obtains an estimate with a predictable standard deviation, thus leading to error bars following the standard statistical scaling for any quantity evaluated using the reconstructed density matrix [23].

The reliability of the method has been further tested by measuring the growth of the trace distance between the dephased states after the interaction as quantified by Eq. (3) for different values of λ and θ and comparing it with the theoretical prediction. The result is plotted in Fig. 5, where different experimental points are measured along lines with fixed relative weight λ and varying angle θ, as well as vice-versa. The theoretical expression is given by the smooth surface. As it appears the trace distance Eq. (3) lies above zero, thus detect-
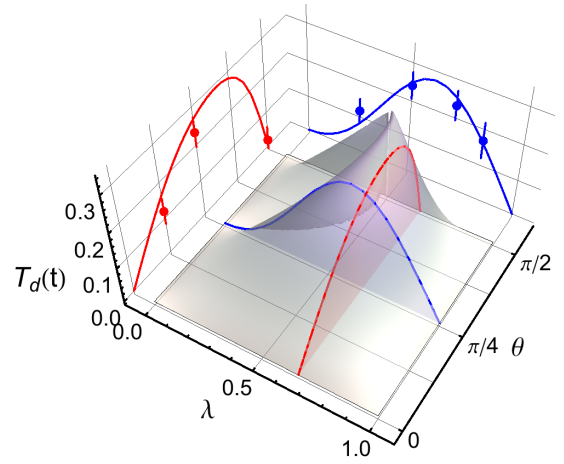

Figure 5. (Color online) Experimental results for the trace distance Eq. (3) corresponding to different values of the parameters λ and θ, as compared to the theoretical prediction given by the smooth surface. The red curve corresponds to $\lambda = 0.65$, while the blue curve is fixed by $\theta = \pi/4$. The experimental points are plotted on the projected curves to improve their visibility.

ing the quantum discord of the state plotted in there left panel of Fig. 3, for all possible values of the parameters λ and θ, apart from a set of measure zero corresponding to the points on the line $\lambda[\cos(2\theta) - 1] = \cos(2\theta)$.

Conclusions and outlook We have suggested and demonstrated a simple all-optical setup to detect and discriminate different kind of SE correlations by performing measurements on the system only. The scheme consists of a two-step procedure. At each step information about the presence and the nature of correlations is extracted by tomographically estimating the distinguishability between system states after the action of suitable global or local quantum operations. In particular, we first assess the presence of quantum discord as quantified by the measurement induced disturbance [10, 19], and then, in the absence of quantum discord, we further determine the factorizability of the state versus the presence of classical correlations, exploiting the connection between initial correlations and growth of trace distance [7]. The successful realization of our procedure is based on the implementation of a dephasing map on the SE state and on the reliable detection of quantum discord. Our procedure can be easily adapted to different experimental settings, the basic requirement being the realization of the dephasing map and the capability to perform state tomography on the sole system. Our results pave the way for reliable detection and discrimination of environments or SE features in systems of interest for quantum technology.

[1] A. S. Holevo, *Probabilistic and statistical aspects of quantum theory* (North-Holland, Amsterdam, 1982)

[2] H.-P. Breuer and F. Petruccione, *The Theory of Open Quantum Systems* (Oxford University Press, Oxford, 2002)

[3] M. Nielsen and I. Chuang, *Quantum Computation and Quantum Information* (Cambridge University Press, Cambridge, 2000)

[4] P. Haikka, S. McEndoo, and S. Maniscalco, Phys. Rev. A **87**, 012127 (2013); M. Borrelli, P. Haikka, G. De Chiara, and S. Maniscalco, Phys. Rev. A **88**, 010101 (2013); M. Gessner, M. Ramm, H. Häffner, A. Buchleitner, H.-P. Breuer, EPL **107**, 40005 (2014)

[5] A. Smirne, S. Cialdi, G. Anelli, M. G. A. Paris, and B. Vacchini, Phys. Rev. A **88**, 012108 (2013)

[6] H.-P. Breuer, E.-M. Laine, and J. Piilo, Phys. Rev. Lett. **103**, 210401 (2009)

[7] E.-M. Laine, J. Piilo, and H.-P. Breuer, EPL **92**, 60010 (2010)

[8] A. Smirne, D. Brivio, S. Cialdi, B. Vacchini, and M. G. A. Paris, Phys. Rev. A **84**, 032112 (2011)

[9] S. Cialdi, D. Brivio, E. Tesio, and M. G. A. Paris, Phys. Rev. A **83**, 042308 (2011)

[10] M. Gessner and H.-P. Breuer, Phys. Rev. Lett. **107**, 180402 (2011)

[11] M. Gessner and H.-P. Breuer, Phys. Rev. A **87**, 042107 (2013)

[12] B. P. Lanyon, P. Jurcevic, C. Hempel, M. Gessner, V. Vedral, R. Blatt, and C. F. Roos, Phys. Rev. Lett. **111**, 100504 (2013)

[13] M. Gessner, M. Ramm, T. Pruttivarasin, A. Buchleitner, H.-P. Breuer, and H. Häffner, Nature Physics **10**, 105 (2014)

[14] K. Modi, A. Brodutch, H. Cable, T. Paterek, and V. Vedral Rev. Mod. Phys. **84**, 1655 (2012); A. Brodutch, Phys. Rev. A **88**, 022307 (2013); D. Girolami & al., Phys. Rev. Lett. **112**, 210401 (2014)

[15] C. A. Fuchs and J. van de Graaf, IEEE Trans. Inf. Th. **45**, 1216 (1999)

[16] S. Cialdi, D. Brivio, and M. G. A. Paris, Phys. Rev. A **81**, 042322 (2010)

[17] C. Zhang, S. Yu, Q. Chen, and C. H. Oh, Phys. Rev. A **84**, 032122 (2011); G. H. Aguilar, O. Jiménez Farias, J. Maziero, R. M. Serra, P. H. Souto Ribeiro, and S. P. Walborn, Phys. Rev. Lett. **108**, 063601 (2012); D. Girolami and G. Adesso, Phys. Rev. Lett. **108**, 150403 (2012)

[18] H. Ollivier and W. H. Zurek, Phys. Rev. Lett. **88**, 017901 (2001); L. Henderson and V. Vedral, J. Phys. A: Math. Gen. **34**, 6899 (2001);

[19] S. Luo, Phys. Rev. A **77**, 022301 (2008)

[20] S. Cialdi, D. Brivio, E. Tesio, and M. G. A. Paris, Phys. Rev. A **84**, 043817 (2011)

[21] S. Cialdi, D. Brivio, A. Tabacchini, A. M. Kadhim, and M. G. A. Paris, Opt. Lett. **37**, 3951 (2012)

[22] D. F. V. James, P. G. Kwiat, W. J. Munro, and A. G. White, Phys. Rev. A **64**, 052312 (2001); K. Banaszek, G. M. D'Ariano, M. G. A. Paris, and M. F. Sacchi, Phys. Rev. A **61**, 010304 (1999)

[23] For each tomographic reconstruction we need 4 acquisitions, each consisting of 30 counts of 1 second. We thus obtain 4 mean counts with the relative standard deviations. Errors on the trace distances are then evaluated by Monte Carlo sampling starting from the experimental results, according to BIPM, IEC, IFCC, ILAC, ISO, IUPAC, IUPAP and OIML 2008 *Evaluation of Measurement Data—Supplement 1 to the Guide to the Expression of Uncertainty in Measurement—Propagation of distributions using a Monte Carlo method* Joint Committee for Guides in Metrology, JCGM 101 http://www.bipm.org/utils/common/documents/jcgm/JCGM_101_2008_E.pdf